# Representation and Self-Similarity of Shapes

Tyng-Luh Liu

Davi Geiger

Robert V. Kohn

Courant Institute
New York University
New York, NY 10012

Courant Institute
New York University
New York, NY 10012

Courant Institute
New York University
New York, NY 10012

## Abstract

*Representing shapes is a significant problem for vision systems that must recognize or classify objects. We derive a representation for a given shape by investigating its self-similarities, and constructing its shape axis(SA) and shape axis tree (SA-tree).*

*We start with a shape, its boundary contour, and two different parameterizations for the contour. To measure its self-similarity we consider matching pairs of points (and their tangents) along the boundary contour, i.e., matching the two parameterizations. The matching, or self-similarity criteria may vary, e.g., co-circularity, parallelism, distance, region homogeneity. The loci of middle points of the pairing contour points are the shape axis and they can be grouped into a unique tree graph, the SA-tree. The shape axis for the co-circularity criteria is compared to the symmetry axis. An interpretation in terms of object parts is also presented.*

## 1 Introduction

With the goal to compare shapes, this paper aims to develop and compute a shape representation.

### 1.1 Motivation: Shape Similarity

Methods to compare two shape contours based on evaluating global deformations [10] tend to be sensitive to occlusion and fail to account for local deformations (such as articulations) since these deformations may change the global appearance of objects considerably while the entire deformation is concentrated in specific points.

A class of methods compares objects by deforming one object into another and evaluating the amount of deformation applied in this process, including [12, 25]. Guaranteed methods, typically, use dynamic programming (time-warping) to register two contours. These are all string (contour) matching algorithms, e.g., [2][6]. The problem with these approaches, as pointed out in [2], is that they do not account for region information and for symmetries (see Figure-1).
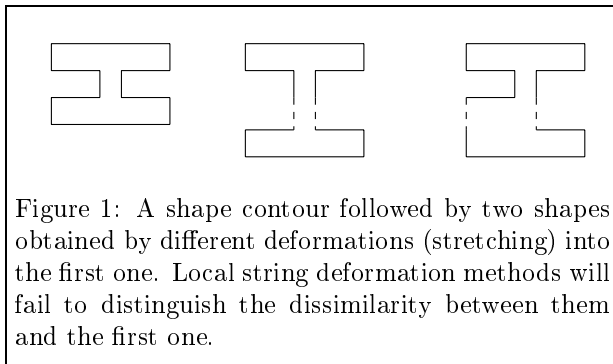


Figure 1: A shape contour followed by two shapes obtained by different deformations (stretching) into the first one. Local string deformation methods will fail to distinguish the dissimilarity between them and the first one.

Our aim is to develop a shape representation of objects that allow similarity measures that account for local deformations, symmetries, and region information. Our representation gives a shape tree axis, where every pair of consecutive nodes (edge) correspond to an object part. The similarity measure between two objects is defined by a tree matching scheme, where the cost of matching edges is the cost of comparing two object parts (local deformations and region information can be accounted.) Tree-matching uses the partial order induced by the trees but is rather more complex than simple string matching algorithms. Moreover, node deletions account for occlusions and moving nodes account for articulations. Figure-2 shows result of using this representation for matching objects.

### 1.2 Shape Representation

Our formulation is a variational one. We start with a shape, its boundary contour. We seek a self-similarity measure to structure the representation of shapes. Our insight is to generate two different parameterizations for the contour and to measure its self-similarity by matching the two parameterizations, i.e., by matching pairs of points (and their tangents) along the boundary contour. The matching, or self-similarity, criteria may vary, e.g., co-circularity, parallelism, distance, region homogeneity. The middle
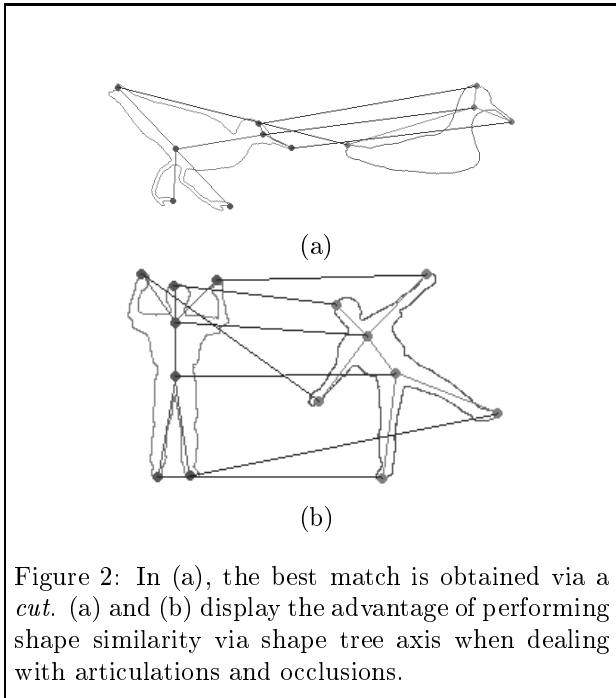
(a)

(b)

Figure 2: In (a), the best match is obtained via a *cut*. (a) and (b) display the advantage of performing shape similarity via shape tree axis when dealing with articulations and occlusions.

point of the pairing contour points gives a shape axis and is guaranteed to yield a tree graph, or a shape tree axis. It is also plausible to extend our work to include curvature sign (convexity). The shape axis for the co-circularity criteria is compared to the symmetry axis. An interpretation in terms of object parts is also presented.

### 1.3   Previous Work

Blum [4] first proposed to represent shapes by their symmetry and thickness [4]. Binford [3] is also a pioneer and bring the attention to generalized cylinders. Other early work include [1][15]. Other work addresses affine transformations [7] and [8], and direct 3D considerations are given in [19]. Pizer et al. [5] have proposed a computational model for object representation via "cores", or regions of high medialness in intensity images [5]. Ogniewicz [16] has given an efficient method based on Voronoi diagrams. Leymarie and Levine [14] have used the grassfire transform (from the psychology literature) which is a simplified description of Siddiqi and Kimia's work [22]. Siddiqi and Kimia's work has given an interesting mathematical formulation based on the reaction-diffusion equation, where the symmetry axis is obtained and described by the development of the shocks (first,second,third, and fourth order ones). They are motivated by their framework for shape analysis via shock-diffusion equations [13]. Our view differs from them on trying to generate a variational formulation for the problem, arguing that

we obtain more control over the criteria to seek the representation (our approach goes beyond the symmetry axis representation and allows for regularization of the solution against small changes in shape). Moreover, it is important to our work that the resulting shape axis give a SA-tree, since our interest is to perform a shape matching based on the tree structure. In Zhu and Yuille's work [26], a system is proposed to recognize and represent flexible objects from their silhouettes. The silhouettes are derived from skeleton extraction and part segmentation using a deformable circle method. Their derivation of the skeleton is of interest, though different from ours, it is not derived from a variational model.

## 2   Variational Matching of Curves

We shall determine the shape axis of a curve by finding a "good match" between the curve and its mirror image. It is convenient to begin, however, with the more general task of finding a "good match" between a pair of curves in the plane.

Consider a pair of parameterized curves $\Gamma = \{x(s) : 0 \leq s \leq 1\}$ and $\tilde{\Gamma} = \{\tilde{x}(t) : 0 \leq t \leq 1\}$. By a *match* between $\Gamma$ and $\tilde{\Gamma}$ we mean a monotone correspondence between the two curves, taking endpoints to endpoints. A match can be represented in several different ways. One representation uses the map $s \mapsto t = t(s)$ such that $x(s)$ corresponds to $\tilde{x}(t(s))$. A second uses the inverse map $t \mapsto s = s(t)$, so $\tilde{x}(t)$ corresponds to $x(s(t))$. A third alternative has the advantage of treating the two curves symmetrically: it specifies a *pair* of monotone functions $s(\sigma)$ and $t(\sigma)$, each defined for $0 \leq \sigma \leq 1$, such that $x(s(\sigma))$ corresponds with $\tilde{x}(t(\sigma))$. (The first two alternatives are special cases, obtained by taking $s(\sigma) = \sigma$ and $t(\sigma) = \sigma$.)

To determine a "good match" we minimize an appropriate variational problem. Concentrating for the moment on our third, more symmetrical representation, the matching energy should have the form

$$\int_0^1 F(x, \tau; \tilde{x}, \tilde{\tau}; s', t') \, d\sigma, \qquad (1)$$

where $\tau = x_s/|x_s|$ and $\tilde{\tau} = \tilde{x}_t/|\tilde{x}_t|$ are the oriented unit tangent vectors to $\Gamma$ and $\tilde{\Gamma}$ at $x(s)$ and $\tilde{x}(t)$. Our notation in (1) is somewhat abbreviated: the integrand must evaluated at the appropriate point $x = x(s(\sigma))$, $\tau = \tau(s(\sigma))$, ..., $s' = ds/d\sigma$, and $t' = dt/d\sigma$.

Our framework imposes two structural conditions on the matching energy density $F$. The first is the symmetry condition

$$F(p, \xi; q, \eta; v, w) = F(q, \eta; p, \xi; w, v),$$

which assures that the notion of "matching" is symmetric, i.e., the two curves $\Gamma$ and $\tilde{\Gamma}$ play equivalent roles. The second is the scaling condition

$$F(p, \xi; q, \eta; \lambda v, \lambda w) = \lambda F(p, \xi; q, \eta; v, w) \quad \text{for all } \lambda > 0,$$

which makes the energy invariant under change-of-variable in $\sigma$:

$$\int F\left(x, \tau; \tilde{x}, \tilde{\tau}; \frac{ds}{d\sigma}, \frac{dt}{d\sigma}\right) d\sigma$$
$$= \int F\left(x, \tau; \tilde{x}, \tilde{\tau}; \frac{ds}{d\sigma}, \frac{dt}{d\sigma}\right) \frac{d\sigma}{d\bar{\sigma}} d\bar{\sigma}$$
$$= \int F\left(x, \tau; \tilde{x}, \tilde{\tau}; \frac{ds}{d\sigma}\frac{d\sigma}{d\bar{\sigma}}, \frac{dt}{d\sigma}\frac{d\sigma}{d\bar{\sigma}}\right) d\bar{\sigma}$$
$$= \int F\left(x, \tau; \tilde{x}, \tilde{\tau}; \frac{ds}{d\bar{\sigma}}, \frac{dt}{d\bar{\sigma}}\right) d\bar{\sigma}.$$

This assures that the energy depends only on the match, i.e., the correspondence between $s = s(\sigma)$ and $t = t(\sigma)$, and not on the specific choice of maps $\sigma \mapsto s(\sigma)$ and $\sigma \mapsto t(\sigma)$.

We want our notion of "match" to be geometric, so it is natural to require invariance under translation and rotation:

$F(p, \xi; q, \eta; v, w)$ depends on $p,q$ only through $p - q$,

and

$$F(Rp, R\xi; Rq, R\eta; v, w) = F(p, \xi; q, \eta; v, w),$$

for every orientation-preserving rotation $R$. These assure that applying the same rigid motion to $\Gamma$ and $\tilde{\Gamma}$ leaves the energy of their match unchanged. Invariance under scaling is too much to ask, but it is natural to ask that

$$F(\lambda p, \xi; \lambda q, \eta; v, w) = g(\lambda)F(p, \xi; q, \eta; v, w) \quad \text{for } \lambda > 0,$$

for some function $g(\lambda)$. Thus scaling $\Gamma$ and $\tilde{\Gamma}$ by a common factor $\lambda$ changes the energy of match by a known amount $g(\lambda)$.

These restrictions leave still considerable freedom. The particular choice of $F$ should depend, of course, on the type of match one seeks.

## 2.1 Similarity Criteria

Various similarity/symmetry criteria can be considered, e.g., co-circularity, parallelism, distance, region homogeneity.
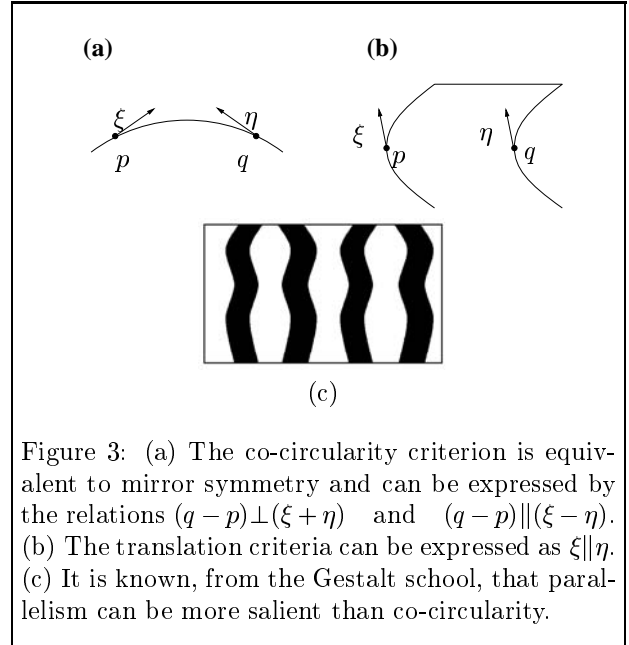


Figure 3: (a) The co-circularity criterion is equivalent to mirror symmetry and can be expressed by the relations $(q - p)\perp(\xi + \eta)$ and $(q - p)\|(\xi - \eta)$. (b) The translation criteria can be expressed as $\xi\|\eta$. (c) It is known, from the Gestalt school, that parallelism can be more salient than co-circularity.

**Co-Circularity or Mirror Symmetry:** We focus on mirror symmetry, i.e., co-circularity, and want $F(p, \xi; q, \eta; v, w)$ to favor

$$(q - p)\perp(\xi + \eta) \quad \text{and} \quad (q - p)\|(\xi - \eta)$$

In other words $F$ favors *co-circularity* – the existence of a circle passing through $p$ and $q$ with tangents $\xi$ at $p$ and $\eta$ at $q$ (see Figure-3). It is also natural to favor $v = w$, so that there are no stretchings, and to favor $p = q$ so that elements are matched when they are close. Two possible choices of $F$'s are

$$F^{(1)}(p, \xi; q, \eta; v, w) = \left[(q - p) \cdot (\xi + \eta)\right]^2 (v + w) + \left[(q - p) \cdot (\xi - \eta)^\perp\right]^2 (v + w) + c|v - w||p - q|^2$$

and

$$F^{(2)}(p, \xi; q, \eta; v, w) = \frac{\left[(q - p) \cdot (\xi v + \eta w)\right]^2}{v + w} + \frac{\left[(q - p) \cdot (\xi v - \eta w)^\perp\right]^2}{v + w} + c\frac{|p - q|^2|v - w|^2}{v + w},$$

where $c$ is a positive constant. We chose the latter form, somewhat arbitrarily (from previous work ([2])), for the examples in this paper.

In practice it is often convenient to use a less symmetric viewpoint, specifying the match by a correspondence $t = t(s)$. This is equivalent to taking

$\sigma(s) = s$, so the matching energy becomes

$$\int_0^1 F\left(x(s), \tau(s); \tilde{x}(t(s)), \tilde{\tau}(t(s)); 1, \frac{dt}{ds}\right) ds.$$

With $F = F^{(2)}$ this amounts to

$$
\begin{aligned}
E[t(s)] & \\
= \int_0^1 \Bigg\{ & \frac{[(x(s) - \tilde{x}(t(s))) \cdot (\tau(s) + \tilde{\tau}(t(s))t'(s))]^2}{1 + t'(s)} \\
& + \frac{[(x(s) - \tilde{x}(t(s))) \cdot (\tau(s) - \tilde{\tau}(t(s))t'(s))^{\perp}]^2}{1 + t'(s)} \\
& + c|x(s) - \tilde{x}(t(s))|^2 \frac{|1 - t'(s)|^2}{1 + t'(s)} \Bigg\} ds,
\end{aligned}
\tag{2}
$$

where $\tau(s)$ and $\tilde{\tau}(t)$ are the unit tangent vectors at $x(s)$ and $\tilde{x}(t)$ respectively.

**Translation:**   Other criteria may also be favorable, and translation is one frequently interesting to be considered (see Figure-3(b)). For translative symmetry, we have experimented with the following energy.

$$
\begin{aligned}
E[t(s)] = \int_0^1 \Bigg\{ & \frac{[|x(s) - \tilde{x}(t(s))|^2 \cdot |\tau(s) - \tilde{\tau}(t(s))t'(s)|^2]}{1 + t'(s)} \\
& + c|x(s) - \tilde{x}(t(s))|^2 \frac{|1 - t'(s)|^2}{1 + t'(s)} \Bigg\} ds.
\end{aligned}
$$

## 2.2   Matching a Curve with Itself

We turn now to our real goal – determining the self-similarity of a closed curve $\Gamma$. Locally, our notion of "good match" is the one introduced above. Globally, however, the situation is different because we now permit discontinuities. The matches considered in this section are only *piecewise* continuous and monotone.

To explain our new notion of "match" more precisely, consider a simple closed curve $\Gamma$ in the plane, parameterized monotonically by $x(s)$, $0 \le s \le 1$, with $x(0) = x(1)$. Extending $x(s)$ periodically, we may consider it to be defined for all $s \in R$, with $x(s+1) = x(s)$. Let $\tilde{\Gamma}$ be "the same curve traced backwards," parameterized by $\tilde{x}(t) = x(1-t)$ (see Figure-4). Notice that $\tilde{x}$ is again defined for all $t$, periodic with period 1.

A match between $\Gamma$ and $\tilde{\Gamma}$ can be represented as a binary function $\mu(s,t)$:

$$\mu(s,t) = \begin{cases} 1 & \text{if } x(s) \text{ corresponds to } \tilde{x}(t) = x(1-t) \\ 0 & \text{otherwise.} \end{cases}$$

We visualize the match by plotting the points in the $s, t$ plane where $\mu(s,t) = 1$ (see Figure-5).
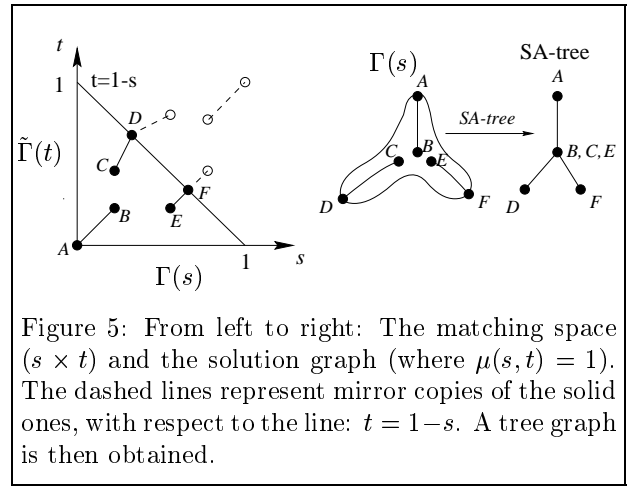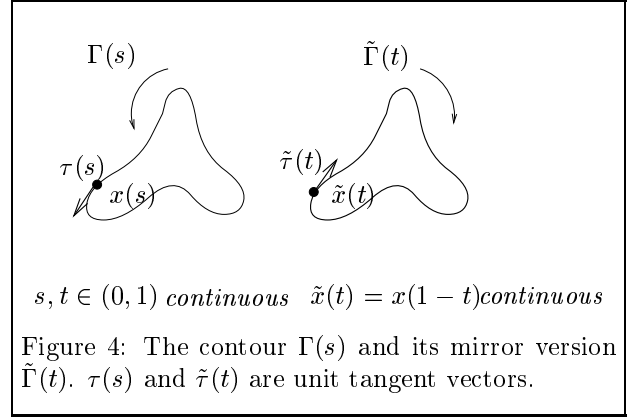


$s, t \in (0,1)$ *continuous*   $\tilde{x}(t) = x(1-t) continuous$

Figure 4: The contour $\Gamma(s)$ and its mirror version $\tilde{\Gamma}(t)$. $\tau(s)$ and $\tilde{\tau}(t)$ are unit tangent vectors.



Figure 5: From left to right: The matching space $(s \times t)$ and the solution graph (where $\mu(s,t) = 1$). The dashed lines represent mirror copies of the solid ones, with respect to the line: $t = 1-s$. A tree graph is then obtained.

There are some structural conditions every match must satisfy. First, to respect the periodicity of $x(s)$ we require

$$\mu(s,t) = \mu(s+1,t) = \mu(s,t+1) \quad \text{for all } s,t. \tag{3}$$

Second, to make $\Gamma$ and $\tilde{\Gamma}$ play equivalent roles we require that

$$x(s) \text{ corresponds with } \tilde{x}(t) = x(1-t)$$
$$\Updownarrow$$
$$\tilde{x}(t) = x(1-t) \text{ corresponds with } x(s).$$

This amounts to

$$\mu(s,t) = \mu(1-t, 1-s); \tag{4}$$

Thus, the plot of $\mu$ must be symmetric about the line $t = 1 - s$. Third, the correspondence must be monotone and continuous except for finitely many jumps, and aside from the jumps every point on $\Gamma$ must have a unique correspondent on $\tilde{\Gamma}$. In other

words, the plot of $\mu$, restricted to the unit square $[0, 1] \times [0.1]$, must consist of finitely many monotone graphs; moreover it should cover each axis exactly once (except for jumps) (see Figure-5).

Every match $\mu$ determines a collection of proposed shape axis, by the rule

$$\mu(s, t) = 1 \Leftrightarrow x(s) \text{ corresponds to } \tilde{x}(t) = x(1 - t)$$

$$\Longleftrightarrow \frac{x(s) + x(1 - t)}{2} \text{ belongs to a shape axis.}$$

Where the plot of $\mu$ is discontinuous, so is the associated shape axis. We call such discontinuities *bifurcations* of the shape axis. Where the plot of $\mu$ crosses the line $t = 1 - s$ the points $x(s)$ and $x(1 - t)$ are identical and the associated shape axis meets $\Gamma$. We call these points the *leaves* of the shape axis.

Of course, to detect the real symmetries of the figure we cannot use just any match – we must use a good one. Each continuous portion of the match is assigned an energy by the analysis of the last section. The total energy is obtained by adding these contributions, then adjoining "jump energies" associated with the discontinuities.

It is frequently convenient to view the plot of $\mu$ as the graph of a piecewise monotone function $t(s)$. Then (4) becomes the condition

$$t(1 - s) = 1 - t(s).$$

In practice the curve $\Gamma$ is given discretely, as a sequence of $N$ points. The data determine $x(s)$ at $s_j = j\Delta s$ with $\Delta s = 1/N$, and $x(s)$ is determined at other points by interpolation. A match $t = t(s)$ between a piece of $\Gamma$ and a piece of $\tilde{\Gamma}$ is determined by specifying $t(s_j)$ for the relevant values of $s_j$. Discretizing the functional introduced in (2) and including the cost of the jumps, the discrete matching energy becomes:

$$E[t(s)]$$
$$= \sum_{s=0,+\Delta s}^{N-1} \left\{ \frac{[(x(s) - \tilde{x}(t(s))) \cdot (\tau(s) + \tilde{\tau}(t(s))t'(s, \Delta s))]^2}{1 + t'(s, \Delta s)} \right.$$
$$+ \frac{[(x(s) - \tilde{x}(t(s))) \cdot (\tau(s) - \tilde{\tau}(t(s))t'(s, \Delta s))^\perp]^2}{1 + t'(s, \Delta s)}$$
$$\left. + c|x(s) - \tilde{x}(t(s))|^2 \frac{|1 - t'(s, \Delta s)|^2}{1 + t'(s, \Delta s)} \right\} \Delta s$$
$$+ \sum_{jumps} \text{Jump Cost}$$

$$(5)$$

where $t'(s, \Delta s) = \frac{t(s + \Delta s) - t(s)}{\Delta s}$. The last term is interpreted as follows: at a jump, the values $t(s+) = \lim_{\delta \to 0} t(s + \delta)$ and $t(s-) = \lim_{\delta \to 0} t(s - \delta)$ are different. The associated jump cost can be a function of $|t(s+) - t(s-)|$. In practice we have used a constant cost for jumps. Our "jumps" amount to the vertical discontinuities one sees in the plot of $\mu$ (see Figure-5). There is no need to handle the horizontal jumps separately because they are in one-to-one correspondence with the vertical ones, on account of the symmetry (4).

## 3 SA Solution and SA-tree Formation

To find the shape axis, we adopt the discretized model (5) where we can list all possible solutions and then are guaranteed to obtain the optimal solution. The solution space is rather large because of all possible bifurcations. To reduce the complexity we have considered using feature points, a small subset of all contour points of $\Gamma$. However, this is not critical to our approach. Our approach is to first develop an algorithm to represent the solution space as a *solution tree* of which each path, from the root to a leaf, corresponds to an SA solution. Then, we can take advantage of the tree structure and apply a shortest path (Dijkstra's) algorithm.

Given a contour $\Gamma$ and a set of feature points $\{p_s, s = 0, ..., n\}$, let $S$ be the solution tree for finding SA with possible bifurcations. Since any bifurcation in an SA is caused by discontinuities of $t(s)$, this implies that all possible SA (or correspondences) can be derived as follows: during the process of matching $\Gamma$ and $\tilde{\Gamma}$, we always move continuously along $\Gamma$ in the $s \nearrow$ (increasing) direction but for $\tilde{\Gamma}$, we can make jump back and forth to one of those feature points starting an unmatched contour segment. In this way, we can exploit all possible bifurcations and to construct a complete solution tree.

### 3.1 Constructing a Shape-Axis Tree

We now show how to go from an SA solution to an SA-tree and derive the object parts. The SA solution, $t(s)$, is a piecewise monotonic function. Let us refer to each monotonic piece as a segment.

For each segment a square box is constructed with one vertex (the bottom left one) being given by the end point of the segment and the other opposite vertex being given by its mirror version (see Figure-6). Note that segments that reach the mirror line ($t = 1 - s$) will create a box of size zero, or to be more precise one point size, the end point of the segment reaching the mirror line. A tree, or box-tree, can then be created according to the nesting parent-child relations among all boxes.

**Leaf nodes:** The box leaves are the ones that have one point size, the ones that correspond to end-points reaching the mirror line. These are the leaf nodes, or *Leaf(T)*, where $T$ represents the tree. Moreover, the origin $(s,t) = (0,0)$ is also in *Leaf(T)*. This asymmetry is artificial and can be be better understood when reminded that the graph $\mu(s,t) = 1$ is periodic (3).

**Bifurcation nodes:** Now we are left to construct the bifurcation nodes of SA-tree $T$, represented by *Bifurcation(T)*. For a non-leaf box, say $\mathcal{B}$, we consider all segments in the region between box $\mathcal{B}$ and all its child boxes (e.g., the shaded region shown in Figure-6). A bifurcation can then be formed by grouping the vertex defining box $\mathcal{B}$ (end-point of a segment) with the start-points of the segments in the region. The set *Bifurcation(T)* can be derived by visiting every box in the box-tree with the grouping criteria just described (see Figures 6).

**Object parts:** We have now a language for defining object parts, where two consecutive nodes of the tree correspond to an object part. How much our definition can really describe object parts is still subject of further investigation.

## 4 Results

Experimental results on SA and SA-tree detection are shown in Figure-7.

## Acknowledgments

## References

[1] H. Asada and M. Brady, "The curvature primal sketch", *IEEE PAMI*, Vol. 5, pp. 2–14, 1983.

[2] R. Basri, L. Costa, D. Geiger and D. Jacobs, "Determining the Similarity of Deformable Shapes", *Physics Based Modeling Workshop in Computer Vision*, 1995.

[3] T. O. Binford, "Visual perception by computer," *IEEE Conference on Systems and Control*, December 1971.

[4] H. Blum, "Biological Shape and Visual Science", *J. of Theoretical Biology*, **38**:205-287, 1973.

[5] C.A. Burbeck and S.M. Pizer, "Object representation by cores: Identifying and representing primitive spatial regions.", *Vision Res.*, Vol. 35, 1995.

[6] Y. Gdalyahu and D. Weinshall, "Measures for Silhouettes Resemblance and Representative Silhouettes of Curved Objects", *4th ECCV*, Cambridge, UK, April 1996.

[7] R. Fawcett, A. Zisserman, J.M. Brady, "Extracting Structure from an Affine View of a 3D Point Set with One or 2 Bilateral Symmetries," IVC(12), No. 9, pp. 615-622, November 1994.

[8] P. Giblin and G. Sapiro "Affine invariant symmetry sets and skew symmetry," *ICCV98*, Bombay, India, January 1998.

[9] Hildreth, E., 1983, *The Measurement of Visual Motion*, MIT Press, Cambridge.
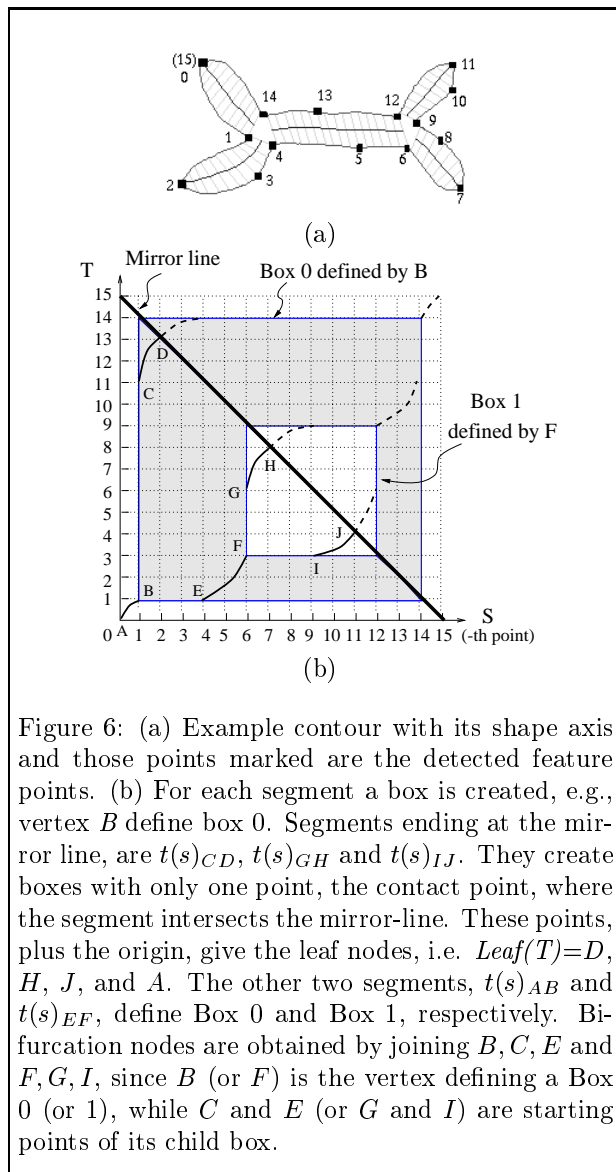


Figure 6: (a) Example contour with its shape axis and those points marked are the detected feature points. (b) For each segment a box is created, e.g., vertex $B$ define box 0. Segments ending at the mirror line, are $t(s)_{CD}$, $t(s)_{GH}$ and $t(s)_{IJ}$. They create boxes with only one point, the contact point, where the segment intersects the mirror-line. These points, plus the origin, give the leaf nodes, i.e. *Leaf(T)=D*, $H$, $J$, and $A$. The other two segments, $t(s)_{AB}$ and $t(s)_{EF}$, define Box 0 and Box 1, respectively. Bifurcation nodes are obtained by joining $B, C, E$ and $F, G, I$, since $B$ (or $F$) is the vertex defining a Box 0 (or 1), while $C$ and $E$ (or $G$ and $I$) are starting points of its child box.

[10] Huttenlocher, D., G. Klanderman, and W. Rucklidge, 1993, "Comparing Images Using the Hausdorff Distance," *IEEE PAMI*, **15**(9):850-863.

[11] D. P. Huttenlocher and S. Ullman, "Object Recognition using Alignment", *ICCV87*, pp. 102-111, 1987.

[12] Kass, M., A. Witkin, and D. Terzopoulos, 1988, "Snakes: Active Contour Models," *Int. J. Comp. Vis.***1**(4):321-331.

[13] B. Kimia, A. Tannenbaum, S. Zucker, 1995. Shapes, Shocks, and Deformations I: The components of two-dimensional shape and the reaction-diffusion space", *Int. J. Comp. Vis.***1**: 189-224,.

[14] F. Leymarie and M.D. Levine. "Simulating the grass-fire transform using an active contour model." *IEEE PAMI*, **14**(1), January 1992.

[15] R. Nevatia and T. O. Binford, "Description and recognition of curved objects," *Artificial Intelligence*, Vol. 8, pp. 77–98, 1977.

[16] R.L. Ogniewicz, *Discrete Voronoi Skeletons*, Hartung-Gorre, 1993.

[17] S. Parent and S. W. Zucker, "Trace inference, curvature consistency and curve detection", *IEEE PAMI*, Vol. 11, No. 8, pp. 823-839, 1989.

[18] A. Pentland, "Recognition by Parts." *ICCV87*:612-620, 1987.

[19] J. Ponce, and O. D. Faugeras, "An Object Centered Hierarchical Representation for 3D Objects: The Prism Tree", *CVGIP*(38), No. 1, April 1987, pp. 1-28.

[20] S.M. Pizer, W.R. Oliver and S.H. Bloomberg, "Hierarchical Shape Description via the Multiresolution Symmetric Axis Transform", *IEEE PAMI*, Vol. 9, No. 4, July 1987.

[21] D. Shasha, J. Wang and K. Zhang, "Exact and Approximate Algorithm for Unordered Tree Matching", *IEEE Trans. Systems, Man, and Cybernetics*, **24**, (4), pp. 668-678, 1994.

[22] K. Siddiqi and B.B. Kimia, "Parts of Visual Form: Computational Aspects", *IEEE PAMI*, Vol. 17, No. 3, pp. 239-251, March, 1995.

[23] K. Siddiqi and B.B. Kimia, " A Shock Grammar for Recognition", *CVPR96*, pp. 507-513, 1996.

[24] D. Terzopolous, A. Witkin, and. M Kass. Symmetry-seeking models and 3D object recovery. *Int. J. Comput. Vision*. 1, 211-221. 1987.

[25] S. Ullman, "Aligning Pictorial Descriptions: An Approach to Object Recognition," *Cognition* **32**(3):193-254, 1989.

[26] S.C. Zhu and A.Yuille, "FORMS: a Flexible Object Recognition and Modeling System", *ICCV95*, 1995.
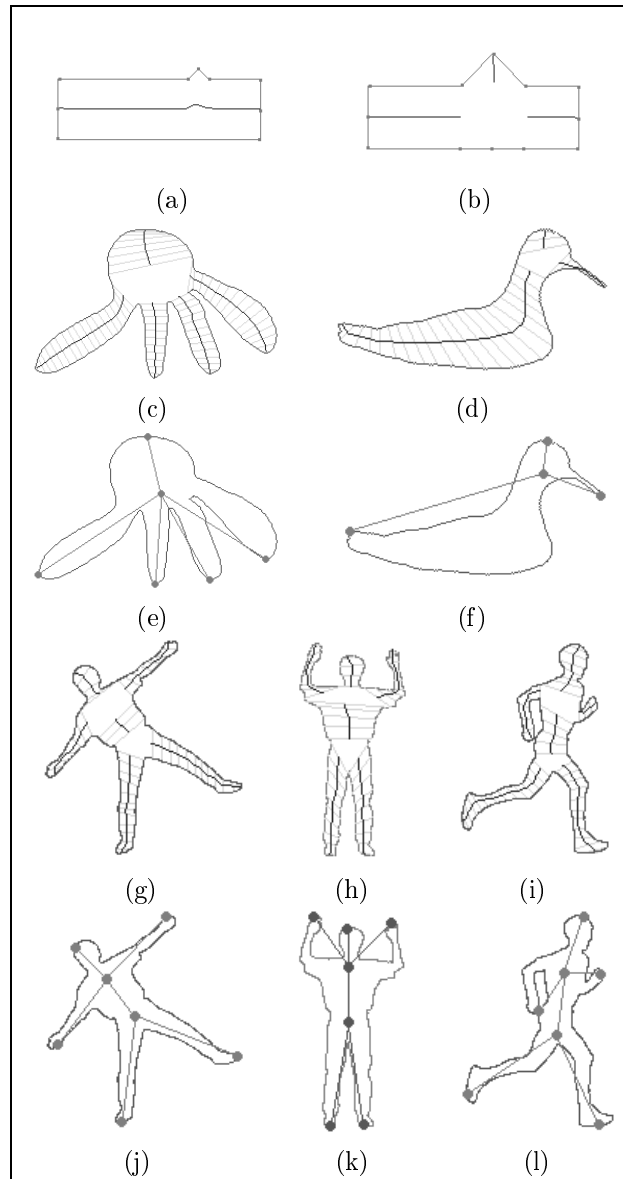
Figure 7: Examples of the SA and SA-tree finding. The original contour and the SA detected with the correspondence matching are shown in (c), (d), (g), (h) and (i). The automatically generated SA-trees are shown in (e), (f), (j), (k) and (l). In (a) and (b), we experiment the effects of boundary perturbation. When the perturbation becomes significant, it will form a part and lead to a bifurcation.